

# Chaos in the Electric Curtain

Owen Myers  
Materials Science Program  
University of Vermont  
Burlington, Vermont 05405  
Email: Oweenm@gmail.com

Junru Wu, Ph.D.  
Department of Physics  
Materials Science Program  
University of Vermont  
Burlington, Vermont 05405  
Email: Jun-Ru.Wu@uvm.edu  
Web Page:  
<http://www.uvm.edu/jwu/Wu.html>

Jeffrey Marshall Ph.D.  
School of Engineering  
University of Vermont  
Burlington, Vermont 05405  
Email: JMasha1.edu  
Web Page:  
<http://www.cems.uvm.edu/jeffm/Research>

**Abstract**—The Electric Curtain (EC) consists of a series of parallel electrodes embedded in a dielectric surface driven by a multiphase alternating electric (AC) voltage source. The EC can transport particles of a variety of materials, and it shows significant promise for dust mitigation and separation applications with charged particles. In this paper, we use a simple mathematical model to demonstrate interesting chaotic behavior of the particles in a EC field. We have identified multiple mode bifurcations as well as the onset of chaotic dynamics of particle motion based on analysis of phase-plane plots, bifurcation diagrams and Poincaré sections. These bifurcations lead to abrupt changes in particle transport properties, such as average translation velocity and elevation height. It may be possible to utilize this information to better understand and control particle transport and/or separation efficiency on the EC by manipulating key physical parameters to trigger or avoid bifurcations. We have further investigated some particle trajectories in phase space when they are on the surface of the EC and briefly describe some interesting behavior of the out-of-plane particle motion.

## I. INTRODUCTION

The Electric Curtain (EC) was patented in 1974 by Senichi Masuda for particles position manipulation and containment in an electrostatic powder painting application [1]. A simple depiction of the EC is shown in Fig. 1. The EC is a series of parallel electrodes that are often embedded in a dielectric surface. A standing wave electric field can be created above the surface by applying a multiphase AC power source to each of the electrodes, and adjusting the phase of this power source between neighboring electrodes to produce the desired wave form. This technique's primary advantage is its simplicity, allowing variations in the electric field above the surface by changing the phase difference between electrodes or the waveforms of the AC voltage applied to them without having to alter the physical apparatus. Whereas most methods for particle transport or separation break down when the particles become charged, the EC relies on particle charge for its operation. The EC has been examined in the context of many different applications. For example, it has been used for separation of cells in solution [2], separation of different types of by-products from agricultural processes [3], transport of toner particles in photocopying machines [4], mitigation of charged dust build-up for extra-terrestrial exploration of dusty planets and moons [5], and separation of charged particles with

different charge-to-mass ratios using a variety of EC designs [6].

The motion of particles on an electric curtain has been studied both experimentally and computationally by a number of investigators. [7]–[13] These investigations have indicated that particles exhibit various different modes of motion on the electric curtain, and they have illustrated how each of these modes produces net motion of the particles. While we use a similar computational approach to some of these previous papers, the current paper has a substantially different objective. Namely, rather than focusing on the net particle motion, we seek to examine the motion from a dynamical systems point of view. With this approach we work to develop greater insight into sudden changes in the nature of particle transport that is sometimes observed in EC particle transport, such as the intermittent changes in particle motion observed in a discrete-element simulation of particle transport on an inclined EC by Chesnutt and Marshall [14]. The onset of chaotic motion of the particle is particularly of interest to us, given the close relationship of chaotic motion and efficient mixing in particulate and fluid systems [15].

## II. METHODS

Three mathematical models were used by Masuda and Kamimura [16] for determining the electrostatic field above the EC surface. The calculations presented in this paper use the so-called center line charge approximation, in which each electrode is approximated as a thin wire. The electrostatic field is assumed to have a standing wave (2-phase) form, such that the phase difference between adjacent electrodes is  $180^\circ$ . The approximate  $x$ - and  $y$ -components of the electric field for a

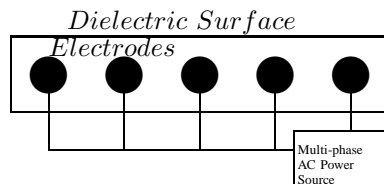


Fig. 1. Side view of electric curtain

2-phase EC are given by

$$E_x = \frac{kQ}{4\pi\epsilon_0} \sum_{n=0}^1 \frac{\sin(kx - n\pi) \cos(\omega t - n\pi)}{\cosh(ky) - \cos(kx - n\pi)} \quad (1)$$

$$E_y = \frac{kQ}{4\pi\epsilon_0} \sum_{n=0}^1 \frac{\sinh(ky) \cos(\omega t - n\pi)}{\cosh(ky) - \cos(kx - n\pi)} \quad (2)$$

where  $Q$  is the charge amplitude on an electrode,  $q$  and  $m$  are the particle charge and mass, respectively,  $k$  is the wave number, and  $\omega$  is the driving frequency [16]. In the cross-sectional plane orthogonal to the electrode axis, the  $x$ - and  $y$ -axes of a Cartesian coordinate system are parallel and perpendicular to the dielectric surface, respectively.

In this initial investigation of bifurcations and chaotic dynamics of the particles on an EC, we have confined attention to a highly simplified mathematical model of the particle dynamics. Primarily we have looked at single particle motion on the EC surface for the case where the particle rolls on the dielectric surface of the EC. This one-dimensional (1D) model offers the advantage of simple phase diagrams and system analysis. We have also performed a preliminary investigation of two-dimensional (2D) particle dynamics on the EC, for which case the particle is allowed to rise off the dielectric surface. In both cases, Poincaré sections are used to simplify the phase space and search for underlying order. In the one-dimensional case, we have also looked for the onset of chaos through a sequence of period doubling.

Dissipative forces are included in both the one- and two-dimensional models. For the 1D case, particles roll along the dielectric surface, so the dissipative forces arise from both rolling resistance and viscous fluid force (Stokes drag). Both of these two forces are proportional to the particle velocity [17], so they are combined into one term in the particle equations of motion. In the 2D case, the particle is assumed to be levitated with non-dissipative collisions with the dielectric surface, so the only dissipation comes from fluid drag. The full differential equations governing the particle's trajectory are

$$\frac{d^2x}{dt^2} + \frac{\beta}{m} \frac{dx}{dt} = \sum_{n=0}^1 J \frac{\sin(kx - n\pi) \cos(\omega t - n\pi)}{\cosh(ky) - \cos(kx - n\pi)} \quad (3)$$

$$\frac{d^2y}{dt^2} + \frac{\beta}{m} \frac{dy}{dt} = \sum_{n=0}^1 J \frac{\sinh(ky) \cos(\omega t - n\pi)}{\cosh(ky) - \cos(kx - n\pi)} - g \quad (4)$$

where  $J = kqQ/4m\pi\epsilon_0$  is called the interaction amplitude,  $\beta$  is the damping coefficient,  $m$  is the particle's mass, and  $g$  is the acceleration due to gravity. In the computations presented, the variables are non-dimensionalized to simplify the numerical analysis. The non-dimensionalized variables and parameters are expressed in terms of their dimensional counterparts as

$$\begin{aligned} t' &= \omega t & j &= \frac{k^2 q Q}{4\pi\epsilon_0 m^2 \omega^2} \\ x' &= kx & g' &= \frac{gk}{\omega^2} \\ y' &= ky & \beta' &= \frac{\beta}{m\omega} \end{aligned}$$

The distance between neighboring electrodes is equal to  $\pi$  and the period of oscillation is equal to  $2\pi$ . The equations of motion can then be written in dimensionless form as

$$\frac{d^2x'}{dt'^2} + \beta' \frac{dx'}{dt'} = \sum_{n=0}^1 j \frac{\sin(x' - n\pi) \cos(t' - n\pi)}{\cosh(y') - \cos(x' - n\pi)} \quad (5)$$

$$\frac{d^2y'}{dt'^2} + \beta' \frac{dy'}{dt'} = \sum_{n=0}^1 j \frac{\sinh(y') \cos(t' - n\pi)}{\cosh(y') - \cos(x' - n\pi)} - g' \quad (6)$$

For the 1D case, the value of  $y'$  in equations (5) and (6) is set equal to the centroid position of the rolling particles. The electric field approximation equations (1) and (2) use singular (point) electrodes, and therefore only accurately represent a physical system of cylindrical electrodes at a sufficiently far distance from the electrodes. To insure that the electrodes are considered far from the particles, the dielectric surface is specified to lie at a distance  $y' = 1$  above the plane of the array of electrodes. Various tests have found this to be adequately far so that the point-electrode approximation is well satisfied. Also, in the 1D study we need to consider values of the parameter  $j$  for which the particles remain on the surface, whereas for the 2D tests we wish to select  $j$  such that particles are levitated from the surface, with occasional collisions. The critical value of  $j$  at which particles transition from 1D motion along the surface to 2D motion off of the surface is determined by putting a particle directly above an electrode with a repulsive interaction and solving for when the electrostatic force balances the gravitational force. We can use the non-dimesionalized equations if we solve for the dimensionless ratio  $j/g'$ . This will give us a critical relationship that will define the range of  $j$  that the 1D model is valid. The acceleration balance equation to be solved at the surface directly above an electrode is

$$\sum_{n=0}^1 j \frac{\sinh(y') \cos(t' - n\pi)}{\cosh(y') - \cos(x' - n\pi)} = g' \quad (7)$$

For a particle located over the electrode at  $x' = 0$  the expression simplifies to

$$j \frac{2 \cos(t') \cosh(y')}{\cosh^2(y') - 1} = g' \quad (8)$$

Therefore the inequality

$$\frac{j}{g'} \leq \frac{\cosh^2(y') - 1}{2 \cos(t') \cosh(y')} \quad (9)$$

needs to be satisfied for the particle to remain on the surface. The right hand side of the inequality is minimized when  $\cos(t') = 1$ . Setting  $\cos(t')$  to its maximum value and setting the location of the surface as  $y' = 1$  we find that  $j/g' \approx 0.448$  is the critical ratio that needs to be considered. For these parameters the 1D model is valid if  $j/g' < 0.448$ . In light of this critical relationship we have chosen  $g'$  such that this criterion is satisfied for  $0 < j < 2$ . It follows that the 2D model is appropriate for  $j/g' > 0.448$  and in this paper we report on interesting findings for  $j/g' \approx 3.06$ .

### III. THE ONE DIMENSIONAL ELECTRIC CURTAIN

The 2-phase EC has two fixed points in the electric field, one located above each electrode. A particle placed directly above an electrode in the 1D system therefore does not move even as the field oscillates in time. The stability of the particle at these locations oscillates with the field. When the charge of the electrode has the same sign of as the particle, the fixed point is unstable because of the repulsion, whereas a particle above an electrode of the same sign charge lies in a stable fixed point. Interestingly, chaotic motion is known to occur in systems that have one stable and one unstable fixed point, which suggests that the 1D EC may present interesting dynamics arising from stability oscillation of these fixed points.

For purposes of analysis, it is convenient to express the governing equation (3) for the 1D model as a set of first-order autonomous differential equations. This can be done by defining three variables,  $x_1$ ,  $x_2$ , and  $x_3$ , by  $x_1 = x'$ ,  $x_2 = \frac{dx'}{dt'}$ , and  $x_3 = t'$ . Equation (3) can then be expressed by

$$\begin{aligned}\dot{x}_1 &= x_2 \\ \dot{x}_2 &= \sum_{n=0}^1 j \frac{\sin(x_1 - n\pi) \cos(x_3 - n\pi)}{\cosh(y') - \cos(x_1 - n\pi)} - \beta' x_2 \\ \dot{x}_3 &= 1\end{aligned}\quad (10)$$

When cast in this form, the periodic conditions in time and space ( $x'$ ) can be employed to represent the system dynamics within a bounded region in phase space. In all test cases reported for the 1D EC the damping coefficient  $\beta'$  is set equal to 0.1 for simplicity.

#### A. Poincaré Sections

The trajectory (or orbit) of a particle in the three-dimensional phase space is obtained by plotting the three coordinates  $x_1$ ,  $x_2$ , and  $x_3$ , as shown in Fig. 2. The orbit of the particle in phase space is usually quite dense, and it is not easy to discern much useful information about the system dynamics directly from such a plot. Valuable insight into the system dynamics can be gained by a Poincaré section, which is simply a cross-section of the particle orbit in phase space where we only plot the points for which the particle trajectory is traveling in a specified direction through the plane. Depending on the particular plane and direction selected the shape of the Poincaré section may differ, but certain structural characteristics of the system will tend to remain the same.

A Poincaré section of the orbit shown in Fig. 2 is obtained by plotting a cross section perpendicular to the time axis and parallel to the position and velocity axes. The orbit only travels in one direction in time so we plot every intersection of the orbit shown in Fig. 2 with the plane chosen, which we arbitrarily put at  $t = 0$ . The resulting Poincaré section is shown in Fig. 3. The shape observed in Fig. 3 is an example of a strange attractor. It is characteristic of chaotic systems with underlying order. If one were to zoom in on a particular part of the strange attractor, it would exhibit the property of self similarity, such that the curve repeats itself on ever smaller scales forming a fractal geometry. Associated with any strange

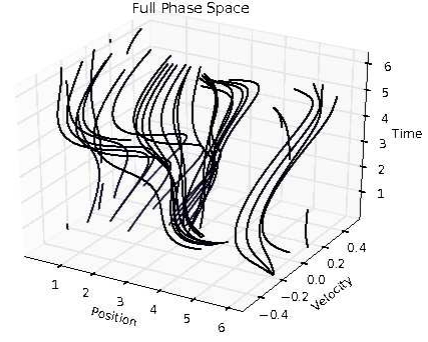


Fig. 2. A particle trajectory periodic in time and space with  $j = .272$

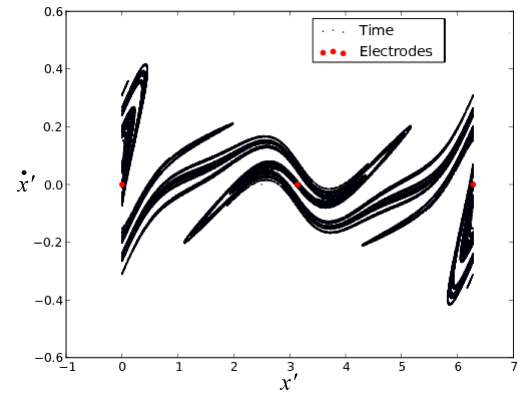


Fig. 3. Poincaré section of trajectory shown in Fig. 2

attractor is a domain of attraction, which are the set of initial conditions that result in a particle approaching an orbit lying within the attractor. A nice feature of this example is that experimentally this particular Poincaré section is easy to make by simply taking a slice at one time throughout each period of the driving frequency, which is the same thing as strobing the system at the driving frequency and then recording the particle velocity and position at each strobe instant. We hope to verify some of our computations by doing just that. One of the benefits of the 1D EC is the ability to view the full phase space graphically. When we look at particle movement off the surface we end up with 5 first-order autonomous equations. We then have to carefully choose how to project and slice the phase space to get useful information.

#### B. Bifurcations

One way to illustrate the system dynamics is with use of a bifurcation diagram, in which the value of one variable (e.g.,  $x'$ ) on the Poincaré diagram is plotted as a function of a system parameter (e.g.,  $j$ ). For small values of  $j$  ( $j < 0.207$ ), the Poincaré diagram consists of a single point, indicating a periodic system with a single period, oscillating in phase with the driving frequency. As the parameter  $j$  is varied, the

corresponding bifurcation plot appears as a single line as long as the period stays in phase with the driving frequency. A period doubling event occurs when the number of distinct frequencies in the oscillations increases by a factor of two. A bifurcation plot for the 1D EC system is shown in Fig. 4 for  $j$  in the interval  $0.200 < j < 0.221$ . A period doubling event is found to occur at  $j \approx 0.207$ , beyond which the Poincaré diagram for the system oscillates between two points, indicating two distinct system frequencies (or period-2 orbit). A second period doubling occurs at  $j = 0.208$ , beyond which the system is characterized by four distinct frequencies (or period-4 orbit). In this second period doubling event the periods appear to change in a discontinuous manner. The period-4 orbit appears to undergo another period doubling event at  $j = 0.210$ , but on closer inspection we find that this is not the case. Instead, the particle trajectory is found to remain a period-4 orbit, but as the value of  $j$  changes the orbits periods are found to discontinuously jump between two sets of values, such that the resulting shape on the bifurcation diagram appears as two dotted lines. Every blank spot in one of these sets of lines coincides with a dot in the other set of lines. As  $j$  is made higher still, the system dynamics transitions back to a period-2 orbit. The sudden jumps in period values and number of periods exhibited by this bifurcation diagram illustrates the very high level of sensitivity exhibited by the electric curtain to changes in system properties in terms of the mode of particle transport.

The bifurcation diagram is plotted in Fig. 5 for the medium-size interval  $0.190 < j < 0.275$  and in Fig. 6 for the large interval  $0.190 < j < 1.700$ . In many systems that exhibit period doubling behaviors, onset of chaos occurs following a cascade of period doubling bifurcations that leads to an infinite period orbit. While numerous period doubling events are apparent in Figs. 4-6, the onset of chaos nevertheless seems to appear quite suddenly near  $j = 0.260$  (Fig. 5). In Fig. 6, it is shown that following a relatively short interval of chaotic motion, the system again returns to a period-2 orbit, and then at much higher values of  $j$  (near  $j = 1.495$ ) the motion again becomes chaotic.

#### IV. TWO DIMENSIONAL ELECTRIC CURTAIN

The 1D EC model loses validity when particles start to hop off of the surface, which occurs for approximately  $j/g' > 0.448$  for the surface at  $y' = 1$ . For the 2D system we include gravity and we set the ratio  $j/g'$  to 3.06 so we are in the regime of out of plane motion. The particular parameters we use for the work shown here are  $j = 0.3$ ,  $g' = 0.1$ ,  $\beta' = 0.03$ . The phase space of the 2D system occupies a 5th order space, which makes analysis considerably harder than for the 1D model. There should be some regime in which the particle leaves the surface but is close enough that the 1D model approximates it. By looking for similarities in Poincaré sections of the two models we hope to determine the full range of  $j/g'$  above 0.448 for which the 1D model is appropriately valid. We are currently working on defining this range in

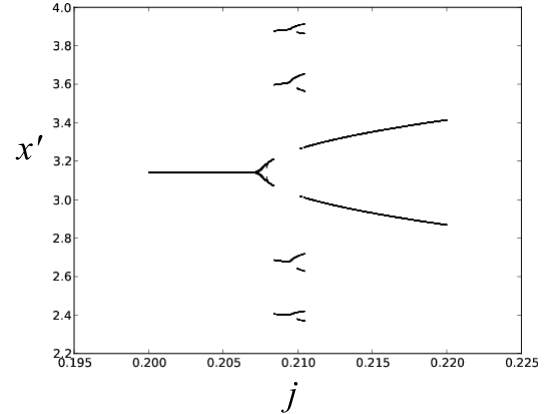


Fig. 4. Bifurcation diagram for  $0.200 < j < 0.221$

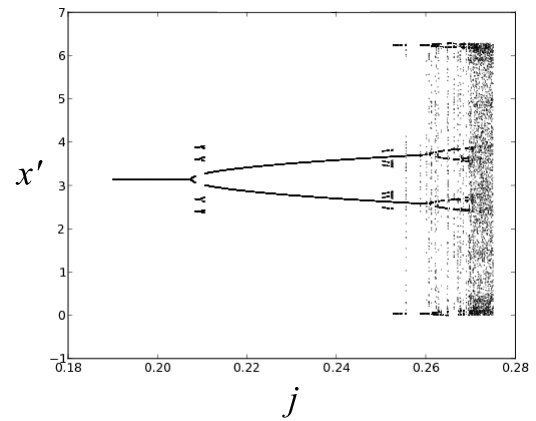


Fig. 5. Bifurcation diagram  $0.190 < j < 0.275$

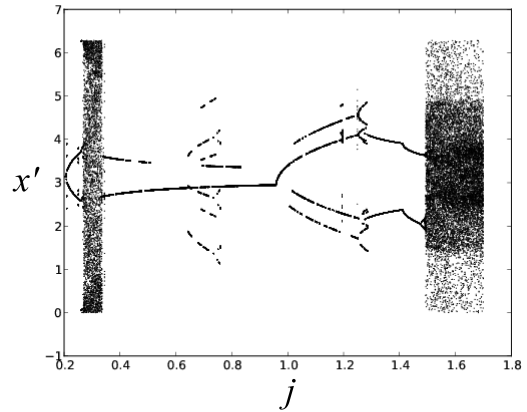


Fig. 6. Bifurcation diagram  $0.190 < j < 1.700$

order to fully exploit the simplicity of the 1D model. This information will be useful in future experimental comparisons.

Poincaré sections of the 2D EC computations are obtained by plotting the particle positions at fixed time increments. Results are shown in Figs 7 and 8. The  $x'$  velocity component

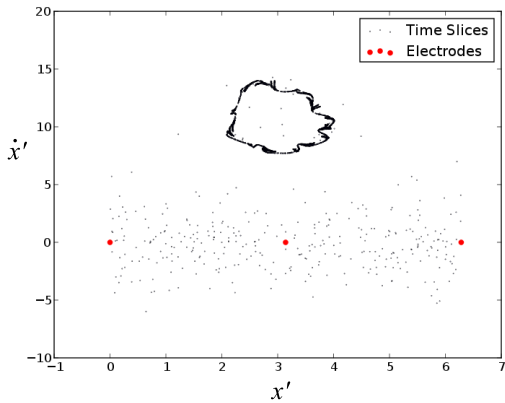


Fig. 7. A Poincaré section parallel to the  $x'$ ,  $\dot{x}'$  phase plane and perpendicular to the time axis.

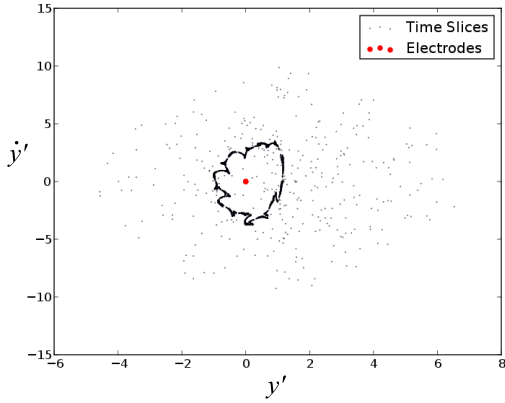


Fig. 8. A Poincaré section parallel to the  $y'$ ,  $\dot{y}'$  phase plane and perpendicular to the time axis.

is plotted against the  $x'$  position of the particle in Fig. 7, and the  $y'$  velocity component is plotted against the  $y'$  position of the particle in Fig. 8. In order to deal with the surface discontinuity that would appear in Fig. 8, after bouncing from the surface the particle motion is folded over the surface position in constructing the Poincaré section. Hence, while a bounced particle is actually located above the surface and moving upward, it is plotted in Fig. 8 as having locations below the dielectric surface with a downward velocity. The particles initially exhibit transient behavior, but over long time settle into a regular pattern characteristic of an attractor. The transient behavior produces scattered points on the Poincaré diagram, and the attractor yields points that form the closed curves in Figs. 7 and 8. The boundary of the attractor appears to fold back on itself at different intervals and to have a complex shape.

## V. CONCLUSION

A dynamical systems study of particle transport on an electric curtain has been initiated, and some preliminary results are reported for both 1D and 2D particle transport. With

use of bifurcation diagrams, we have shown that the system undergoes a series of period doubling bifurcations, which in some cases lead to intervals of chaotic dynamics and in other cases reverts back to a simple finite period orbit. Poincaré sections are plotted which illustrate the presence of strange attractors in both 1D and 2D systems under chaotic transport conditions. We hope to continue our research of the simple 2D model, as well as to explore more complex cases with particle-particle collisions and multiple particles sizes, with the hope that by better understanding the dynamics of such systems we will be better able to design electric curtain devices for optimal particle transport, mixing and separation operations.

## ACKNOWLEDGMENT

This work has been supported by NASA under cooperative agreement number NNX08AZ07A.

## REFERENCES

- [1] S. Masuda, "Booth for electrostatic powder painting with contact type electric field curtain," USA Patent 3 801 869, April, 1974.
- [2] S. Masuda, M. Washizu, and I. Kawabata, "Movement of blood cells in liquid by nonuniform traveling field," *IEEE Transactions on Industry Applications*, vol. 24, pp. 217–222, Mar/Apr 1988.
- [3] L. C. Weiss and D. P. Thibodeaux, "Separation of seed by-products by ac electric field," *JAOCs*, vol. 61, no. 5, pp. 886–890, May 1984.
- [4] F. W. Schmidlin, "Development apparatus," USA Patent 4 647 179, March 3, 1987.
- [5] M. Mazumder, R. Sharma, A. Biris, J. Zhang, C. Calle, and M. Zahn, "Slef-cleaning transparent dust shields for protecting solar panels and other devices," *Particulate Science and Technology*, vol. 25, pp. 5–20, May 2007.
- [6] H. Kawamoto, "Some techniques on electrostatic separation of particle size utilizing electrostatic traveling-wave field," *Journal of Electrostatics*, vol. 66, pp. 220–228, 2008.
- [7] H. Kawamoto, K. Seki, and N. Kuromiya, "Mechanism of travelling-wave transport of particles," *Journal of Physics D: Applied Physics*, vol. 39, pp. 1249–1256, 2006.
- [8] G. Liu and J. Marshall, "Particle transport by standing waves on an electric curtain," *Journal of Electrostatics*, vol. 68, pp. 289–298, 2010.
- [9] Z. Dudzicz, "Recording of dust particle oscillation path inside electric curtain by laser diode apparatus," *Optica Applicata*, vol. 35, pp. 907–912, 2005.
- [10] F. W. Schmidlin, "Modes of traveling wave particle transport and their applications," *Journal of Electrostatics*, vol. 34, pp. 225–244, 1995.
- [11] ——, "A new nonlevitated mode of traveling wave toner transport," *IEEE Transactions on Industry Applications*, vol. 27, pp. 480–487, 1991.
- [12] J. M. Hemstreet, "Velocity distribution on the masuda panel," *Journal of Electrostatics*, vol. 17, pp. 245–254, 1985.
- [13] ——, "Three-phase velocity distribution of lycopodium particles on the masuda panel," *Journal of Electrostatics*, vol. 27, pp. 237–247, Mar 1991.
- [14] *Simulation of Particle Separation on an Inclined Electric Curtain*, Jun 2010.
- [15] J. Ottino, *The Kinematics of Mixing: Stretching, Chaos, and Transport*. Cambridge University Press, 1989.
- [16] S. Masuda and T. Kamimura, "Approximate methods for calculating a non-uniform travelling field," *Journal of Electrostatics*, vol. 1, pp. 351–370, January 1975.
- [17] N. Brilliantov and T. Poschell, "Rolling as a continuing collision," *The European Physical Journal B*, vol. 12, pp. 299–301, 1999.